IJNRD.ORG ISSN : 2456-4184
INTERNATIONAL JOURNAL OF NOVEL RESEARCH AND DEVELOPMENT (IJNRD) | IJNRD.ORG
An International Open Access, Peer-reviewed, Refereed Journal

DUAL SOURCE HYBRID PV-FC INVERTER WITH MICROCONTROLLER GATING CIRCUIT

RAHUL[1], ROHAN S[2], JEETHANAND K J[3], MOHAMMED SAMAQUE[4], Dr KUSUMADEVI G. H.[5]

DEPARTMENT OF ELELCTRICAL AND ELECTRONICS ENGINEERING

Acharya Institute of Technology 2022-2023

ABSTRACT

This paper investigates the design and analysis of a dual source inverter (DSI) for hybrid photovoltaic (PV) and fuel cell (FC) applications. PV cells and FCs are promising renewable energy sources, but each has limitations when used alone, such as intermittent output and low efficiency. [1]A DSI can integrate the two sources to create a hybrid system that provides a continuous and stable power output.[2] In this paper, we designed and simulated a DSI, and analysed its performance in a hybrid system. We used MATLAB/Simulink software to model the DSI and the hybrid system, in a way that the two impedance networks have better power-sharing capabilities. [3] The results showed that the DSI was able to efficiently integrate the PV cells and FCs and improve the overall performance of the hybrid system.

Index Terms: PV-PANNEL, BATTERY, Z-SOURCE, TRANSFORMER

INTRODUCTION

Due to environmental concerns and the availability of non-renewable resources, the demand for renewable energy sources has increased over the past several years. Photovoltaic (PV) cells and fuel cells (FCs) are two of the most promising and extensively utilised renewable energy sources. PV cells and FCs have limitations when used independently, including intermittent output and low efficiency. Combining the two sources into a hybrid system that can provide a continuous and stable power output is one solution. In such hybrid systems, the dual-source inverter (DSI) is a crucial component, as it enables the integration of PV cells and FCs. With such integration, the overall performance of the dual source inverter drastically increases, and proves that its better than the conventional inverters

This project's objective is to design and evaluate a DSI for hybrid PV and FC applications. The undertaking entails modelling the DSI and the hybrid system using MATLAB/Simulink and evaluating the performance of the DSI under different operating conditions. The project's objective is to examine the viability of a DSI for integrating PV cells and FCs to produce a more efficient and dependable hybrid system.

CIRCUIT DIAGRAM AND CALCULATIONS

A. Schematic Diagram

The dual source inverter design is implemented as in [1 As seen in Fig. 1, Z-Source 1 has two transformers in its structure instead of two inductors. These transformers' secondary voltages (Vsec1 and Vsec2) are connected to Z-Source 2

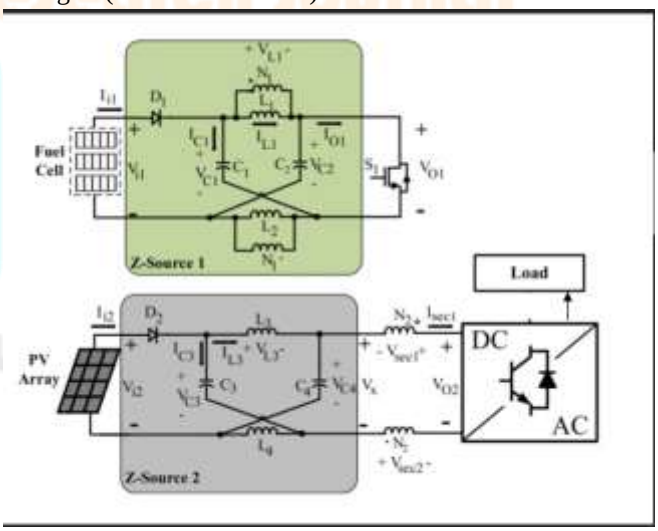

Figure 1

series, and as a result, the inverter's DC-link voltage is equal to VX plus Vsec1 plus Vsec2. The transformers' magnetising inductances serve as Z-Source 1's necessary inductors. The gating circuit for the switches (microcontroller and opt isolator circuitry)

B. Simulation Circuit

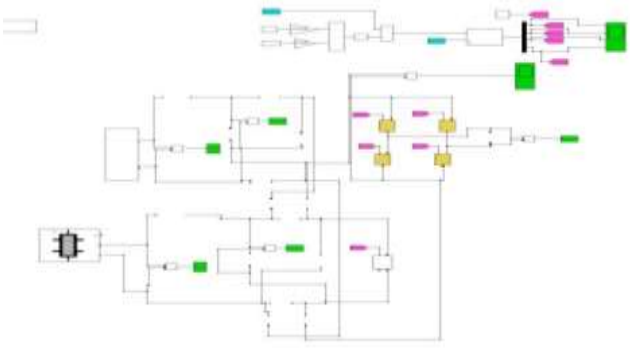

Figure 2

Above is the circuit of the Hybrid Dual Source Inverter. As we can see we use two Z-source inverters for this project. The two Z-source inverters are connected to each other through transformers. We have used two z-source inverters to accommodate both of the inputs, Fuel Cell and Photo-Voltaic cell namely.

C. PIC Microcontroller

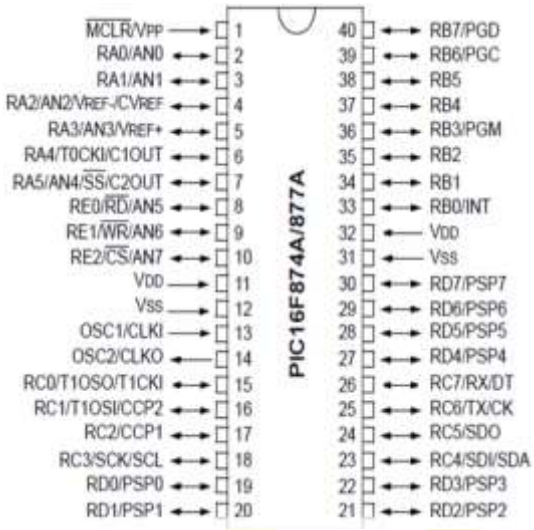

Figure 3- PIC Microcontroller pin diagram

The PIC microcontroller PIC16f877a is one of the most renowned microcontrollers in the industry. This controller is very convenient to use, the coding or programming of this controller is also easier. One of the main advantages is that it can be write-erase as many times as possible because it use FLASH memory technology. It has a total number of 40 pins and there are 33 pins for input and output. PIC16F877A is used in many pic microcontroller projects. PIC16F877A also have many applications in digital electronics circuits.

D. Steady state operation analysis

The analysis of the dual source inverter's steady-state operation is elaborated on in [1]. Due to the symmetry of the circuit, only a portion of the circuit is analysed. Obviously, the behaviour of the other component is identical. Similar relationships exist between the capacitor voltages (VC1 and VC2) and the output voltage (VO1):

$$\frac{V_{C1}}{V_i} = \frac{1 - D_{st1}}{1 - 2D_{st1}}$$

$$\frac{V_{O1}}{V_{i1}} = \frac{1}{1 - 2D_{st1}}$$

where D_{st1} is the duty cycle for Z-Source 1's shoot-through stateWhen S1 is ON (the shoot-through condition for Z-Source 1) and VC1 is applied to the transformer's main winding, the secondary voltage of the transformer, Vsec1, is positive. This is also true for Vsec2 and VC1. When this period of time (Dst1T) is present, Vsec1 is as follows:

$$V_{sec1} = \frac{N_2}{N_1} V_{C1}$$

Due to the volt-second law for the transformers' magnetising inductors, the secondary voltage is negative during non-shoot through time (when S1 is off) and is equal to:

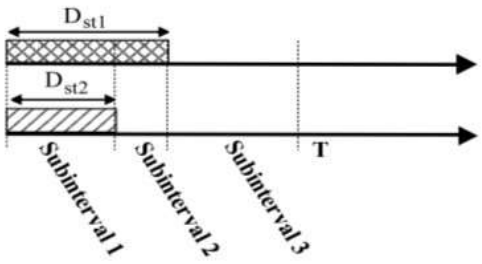

Figure 4- Mode 1 Operation

Two operating modes are defined as illustrated in Fig. 3.3 based on the values of Dst1 and Dst2 and their relative positions in time. The fundamentals of how the converter operates in both modes are discussed in the next section.

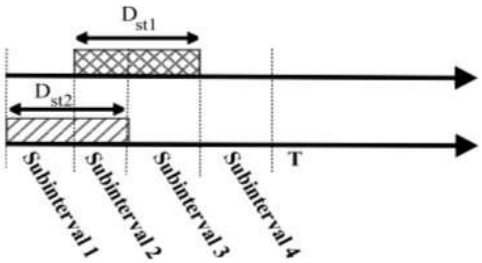

Figure 5- Mode 2 Operation

Operation in mode 1 - [1] gives a thorough explanation of mode-1 operation. Two Z-Source networks simultaneously enter the shoot-through condition in this mode of operation. Shoot-through periods, however, can vary (Fig. 2a). Diode D2 may or may not be conducting during (Dst1 - Dst2)T (subinterval 2), depending on the input voltage levels, the output current level, and the duty cycle values (Dst1 and Dst2). In the next subinterval, it is assumed that all symmetric elements (such transformer turn ratio (n) or L3 and L4 or...) have the same values and behaviours. The analogous circuits for all three converter states in Mode I are shown in Figure 3, along with the actual current directions (red dashed lines) in each circuit branch. As seen in Fig. 3a, in Due to the shoot-through status of both Z-sources at Dst2T (subinterval 1), VL3 = Vc3 + 2Vsec1 = Vc3 + 2nVC1, and V1o2 = 0. When Z-source 2 enters the non-shoot-through state, it produces a value larger than the inductor voltage in a classic Z-source because it is obvious that L3 charges with a value larger than VC1 (in comparison to a classic Z-source). V202= Vi2 2VL3+ 2Vsec1 = Vi2 2VL3 + 2nVC1 when the converter is in subinterval 3 (1 Dst1T), when the converter is in subinterval 2 ((Dst1 Dst2)T), $V_{302} = V_{i2} - 2V_{L3} + 2V_{sec1} = V_{i2} - 2V_{L3} + 2(V_{i1} - V_{C1})$

Because $V_{i1} - V_{C1} < V_{C1}$ so $V^2_{O2} > V^3_{O2}$ In other words, VO2 is a three-level signal that has non-zero values in the other states (subintervals 2 and 3) and is zero when Z-source 2 is in a shoot-through state (subinterval 1). Figure 3.4 shows the shoot-through duty cycles for the converter and VO2.

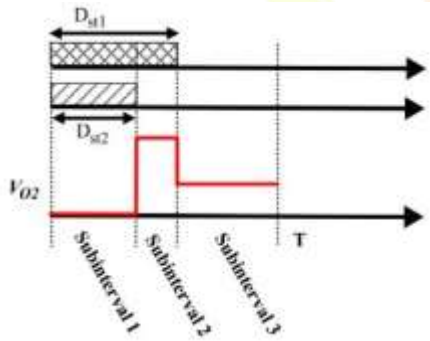

Figure 6 The schematic waveform for V02 in mode-1

Values of the important variables in this Mode will be calculated. Employing volt-second law for inductor L_3 yields:

$(2nV_{C1} + V_{C3})D_{st2} + V_{i2} - V_{C3}(D_{st1} - D_{st2})T + (V_{i2} - V_{C3})($ $V_{C3} = V_{i1} + (1 - D_{st1})T = 0$ Simplifying the above equation using KVL we get Where V^2_{02} and V^3_{02} are the DC link voltages during subintervals 2 and 3 respectively.

The current relations of the system must be derived in the following manner in order to examine the power-sharing between two networks. Given that the average currents of the capacitors are zero during steady state operation, the average values of the currents can be computed as follows:

$$V_{C3} = V_{i1} + \frac{(1 - D_{st2}) \cdot (1 - 2D_{st1})V_{i2}}{2nD_{st2}(1 - D_{st1})}$$

$$V^2_{O2} = V_{i1} + \left(\frac{D_{st2}(1 - 2D_{st1})}{2n(1 - D_{st1})(1 - 2D_{st2})}\right)V_{i2}$$

$$V^3_{O2} = V_{i1} + \left(\frac{D_{st2}(1 - 2D_{st1})}{2n(D_{st1}D_{st2} - D_{st1} + D_{st2})}\right)V_{i2}$$

$$I_{L3} = I_{sec1}$$

$$I_{i1} = I_{L1} + nI_{sec1} = I_{L1} + nI_{L3}$$

$$I_{i2} = I_{L3}$$

$$I_{O1} = nI_{sec1} + I_{L1} = nI_{L3} + I_{L1}$$

According to the circuit operation in this Mode; I_{sec1} can be expressed as above.

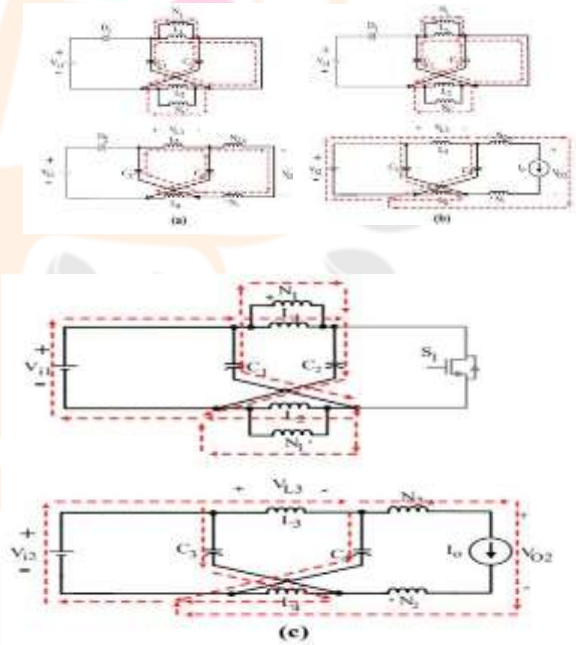

Figure 7- The equivalent circuits for mode-1 for (a) Ds2 T (subinterval 1) (b) (Ds1-Ds2)T (subinterval 2) (c) (1- Ds1)T (subinterval 3)

Operation in Mode-2 - [1] gives a thorough explanation of mode-2 operation. In this mode, the shoot-through condition is initiated by both Z-source networks and ends by different Z-source networks. The flexibility to regulate Z-source 1's contribution to carrying the load is this switching method's main advantage over Mode I. Mode will perform better than Mode if the system wants to deliver the load such that the z-Source 2 should contribute more. When Z-source 1 is in the shoot-through condition and Z-source 2 isn't, as in Mode I, at that precise moment, VO2 is at its highest level. VO2 is

a three-level signal as well. Shoot-through signals and DC-link voltage for this Mode are shown in Figure 3.5.

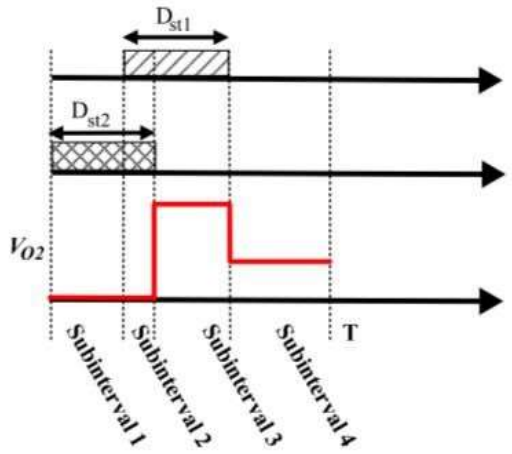

Figure 8- DC link voltage waveform for Mode-2

Subintervals 2, 3, and 4 in this Mode are comparable to subintervals 1, 2, and 3 in Mode, respectively, because equivalent circuits and current directions in this Mode are like those in Mode I. Only subinterval 1 is different from them and is according to Fig 8: If the duty cycle of subinterval 2 is defined as D_{ov}, Similar to Mode I, it can be said:

$$V_{C3} = V_{i1} - \left(\frac{(1 - D_{st2})(1 - 2D_{st1})}{2nD_{ov}(2D_{st2} + D_{st1} - 2D_{ov} - 1)} \right) V_{i2}$$

$$V_{O2}^{3} = V_{i1} - \left(\frac{(1 - 2D_{st1} + D_{st2})(1 - 2D_{st1})}{n(4D_{st2} + 2D_{st1} - 4D_{ov} - 1)} \right) V_{i2}$$

$$V_{O2}^{4} = V_{i1} - \left(\frac{1 - 2D_{st1}}{2n(D_{st1} - 2D_{ov})} \right) V_{i2}$$

Where V3o2 and V4o2 are, respectively, the subintervals 3 and 4 DC link voltages. Similar to Mode I, simultaneous extraction of the active power values generated by Z-sources 1 and 2 is required. The relationships regulating the system in this Mode are calculated and simplified.

$$P_{z1} = V_{i1} \cdot \left(I_{inv}^{3} + I_{inv}^{4} \cdot \left(\frac{2(2D_{ov} - D_{st1})(1 - D_{st1} - D_{st2} + D_{ov})}{(D_{st1} - D_{ov})(1 - D_{st1} - 2D_{st2} + 2D_{ov})} \right) \right)$$

$$P_{z2} = V_{i2} \cdot \left(I_{inv}^{3} + I_{inv}^{4} \cdot \frac{1 - D_{st1} - D_{st2} - D_{ov}}{D_{st1} - D_{ov}} \right)$$

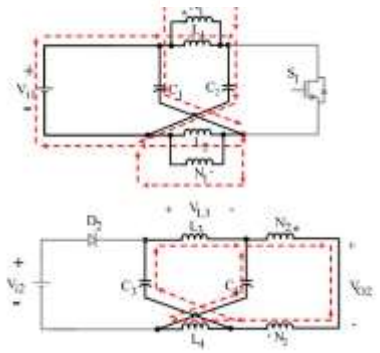

Figure 9- Equivalent converter circuit for subintervals in mode 2

SIMULATION WITH RESULTS

From both the Figure 9 and Figure 10, we can see the output of the two inputs which we are applying to the Hybrid Dual Source Inverter. This gives us the required output to store and give the maximum output with good efficiency. As mentioned before, this Hybrid Dual Source Inverter has good power sharing capability which manages both the inputs simultaneously to give us the maximum output

A. Software Used- MATLAB

The simulation can be done using MATLAB versions 6.1 and higher. Its main user interface consists of a graphical block diagramming tool and a set of block libraries that can be customized. It may be used to drive MATLAB or be programmed from it and enables close connection with the rest of the MATLAB environment.

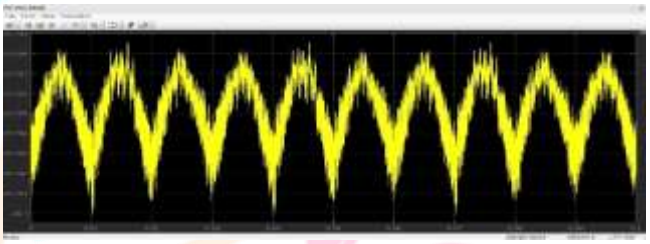

B. Complete Circuit Constructed for the Simulation Description

Figure 11- Output of Photo-Voltaic

To validate the theoretical analysis, the proposed converter is simulated in MATLAB. We simulated the below circuit with the required specifications and built the circuit on MATLAB Simulink Software and executed the same. Connect the Voltage Sources to the Full-Bridge Inverters as shown in the Dual Source Inverter circuit diagram.

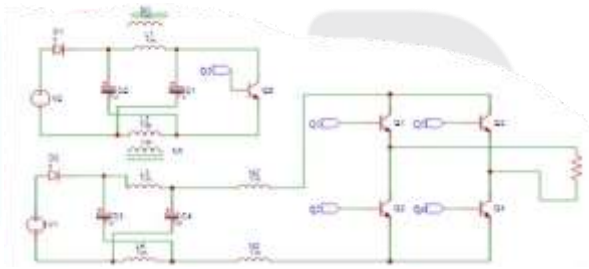

Figure 12- Circuit Diagram

Figure-12 shows the circuit of the Hybrid Dual Source Inverter. As we can see we use two Z-source inverters for this project. The two Z-source inverters are connected to each other through transformers. We have used two z-source inverters to accommodate both inputs, Fuel Cell, and Photo-Voltaic cell namely.

Figure 13 shows the final output of our Dual Source Inverter

Figure 10- Output of Fuel Cell

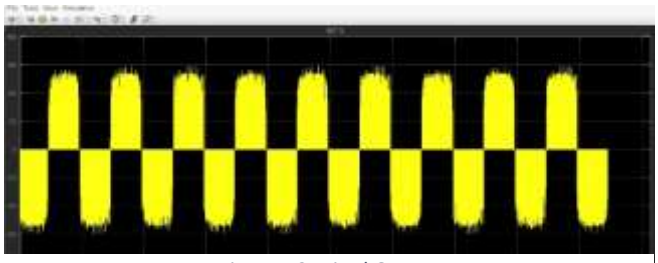

Figure 13- Final Output

on MATLAB Simulink that's needed at all times. Therefore, it is obvious that using a hybrid dual source inverter is much more advantageous than using another type in the overall scheme of things where typically a VSI (Voltage Source Inverter) is used.

In a PWM-based PV-FC HDSI, the output waveform is generated by modulating the width of the pulses of the inverter output voltage. The duty cycle of the PWM waveform is controlled by the modulation index, which determines the amplitude of the output waveform. The phase shift between the two DC sources also affects the shape of the output waveform.

The output voltage of the PV-FC HDSI is regulated to maintain a constant output voltage level. The regulation is achieved by using a control algorithm that adjusts the duty cycle of the PWM waveform based on the output voltage and the reference voltage.

As we can see in the above figure, the output we got is 60V(p-p). After building the hardware prototype, we compared the output of both, the simulation, and the hardware. The output we got in the hardware prototype was 45V RMS value, after converting the RMS into peak value, which is 45*1.414, we got 63.63V(pp) value. Hence confirming the output in both practical and simulation

CONCLUSION

In conclusion, hybrid dual source inverter (HDSI) is a promising technoogy that combines two DC sources to supply power to AC loads. The use of HDSIs has several advantages, such as improved reliability, reduced dependence on a single source, and increased efficiency. The output waveform of an HDSI can be controlled by varying the modulation index and the phase shift between the two DC sources, making it suitable for various applications.

References

[1] A. R. M. M. Majid Ghani Varzaneh, "Dual Source Inverter for Hybrid PV-FC Application".

[2] "Tutorial for programming the microcontroller PIC-16F877A," [Online]. Available: https://deepbluembedded.com/pic-programming-tutorials.

[3] " Datasheet for TLP250 Photocoupler," [Online]. Available: https://toshiba.semicon-storage.com/info/datasheet_en_20190617.pdf?did=16821.

[4] "PIC-16F877A Datasheet," [Online]. Available: www.microchip.com.